Accuracy Improvement Method for Engine Large-scale Assembly Analysis Using Vibration Data During Actual Operation

YASUO KATO[*1] TAKUYA KUMAGAI[*1]
KENYA AJIRO[*2]

Along with an increase in the output of engines, the components in the intake and exhaust systems, such as turbochargers, air coolers, and piping, have become larger, and the intake and exhaust system assemblies have been in many cases mounted overhanging the engine main body as a result. In addition, the increase in the number of parts and couplings in the assembly makes the evaluation of strength against vibration more complicated, so that the accuracy of the analysis is required to be improved. Therefore, in order to establish methods to improve the accuracy of vibration analysis of gas engine intake and exhaust system assemblies, we have clarified processes that are effective in improving the accuracy of the analysis.

1. Introduction

There was a case where an air intake and exhaust system assembly newly designed for the development of a new model suffered vibration-induced damage. The damage stemmed from a discrepancy between the vibration analysis result at the design stage and the actual measurement result after the engine was installed. As a result, to reduce vibration, the design had to be changed by reinforcing parts or adding anti-vibration parts. In response to this, Mitsubishi Heavy Industries Engine & Turbocharger, Ltd. (MHIET)worked to improve the accuracy of the vibration analysis of the intake and exhaust system assembly of the G16NB engine, which experienced the problem. We improved the accuracy of the vibration characteristics of the analytical model by hammering, established a method for calculating analytical input conditions using measured vibration values from actual engine operation. Then we verified that the method can accurately estimate the vibration modes and vibration stresses of intake and exhaust system assemblies. This report describes these results.

2. Summary of G16NB engine

G16NB engine is a new gas engine for power generation that employs a two-stage turbocharger system to achieve the highest level of power generation efficiency in its output range. It has four turbochargers (two low-pressure turbochargers and two high-pressure turbochargers) located at its front side and air coolers (two low-pressure coolers and one high-pressure cooler) placed at the backstream of the first-stage low-pressure turbocharger and the backstream of the second-stage high-pressure turbocharger, respectively, all of which, including the accompanying piping, are mounted in a position that overhangs forward from the engine main body. **Figure 1** shows the intake and exhaust system assembly of the G16NB engine used as an analysis target in this study.

*1 Chief Staff Manager, Engine Engineering Department, Engine & Energy Division, Mitsubishi Heavy Industries Engine & Turbocharger, Ltd.
*2 Engine Engineering Department, Engine & Energy Division, Mitsubishi Heavy Industries Engine & Turbocharger, Ltd.

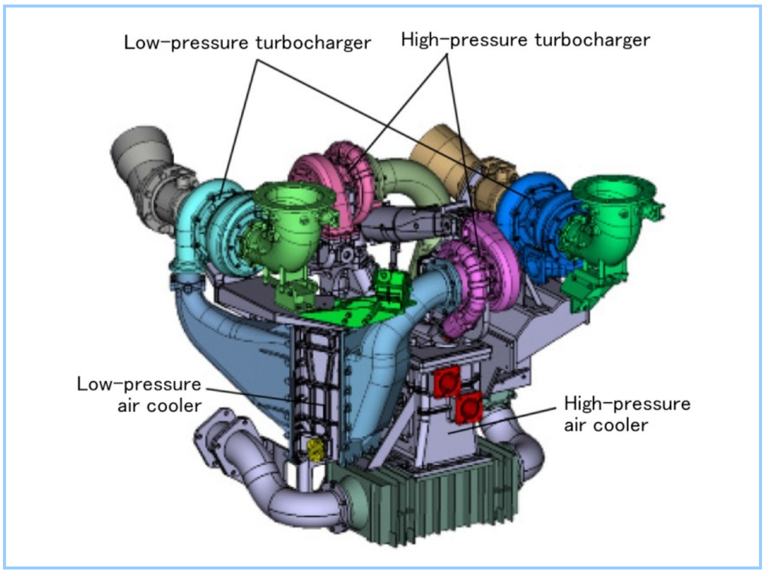

Figure 1 G16NB intake and exhaust system assembly

3. Correlation of FEM model

Figure 2 shows the procedure for improving the accuracy of FEM (Finite Element Method) models.

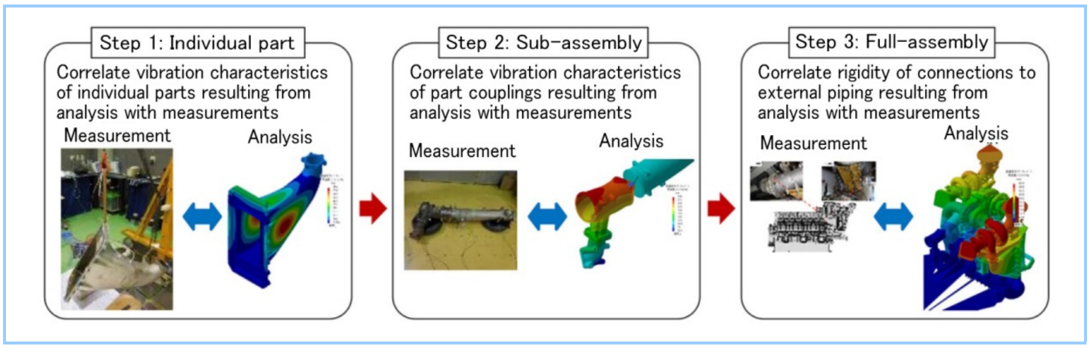

Figure 2 Procedure for improving the accuracy of FEM models

Step 1: We selected individual parts that are considered to have a high affect to the vibration mode of the entire assembly from the components of the intake and exhaust system assembly (**Figure 3**), and performed hammering tests on them to correlate the vibration characteristics of the FEM model with the measurements using the transfer function at the excitation point as an indicator. This correlation was made by adjusting the material properties (material density, Young's modulus, and damping coefficient) (hereafter referred to as correlation). **Figure 4** shows a correlation example of an individual part. (1) The material density was adjusted to match the measured weight, (2) the resonance peak frequency was adjusted by Young's modulus, and (3) the amplitude of the resonance peak was adjusted by the damping coefficient. **Figure 5** shows a comparison of the measured and analyzed natural frequency for the 13 parts for which the individual-part correlation was made. The difference between the measured and analyzed natural frequency was a maximum of 16% in the initial model, but was reduced to about 3% for the sheet metal parts and about 7% for the cast parts as a result of the correlation.

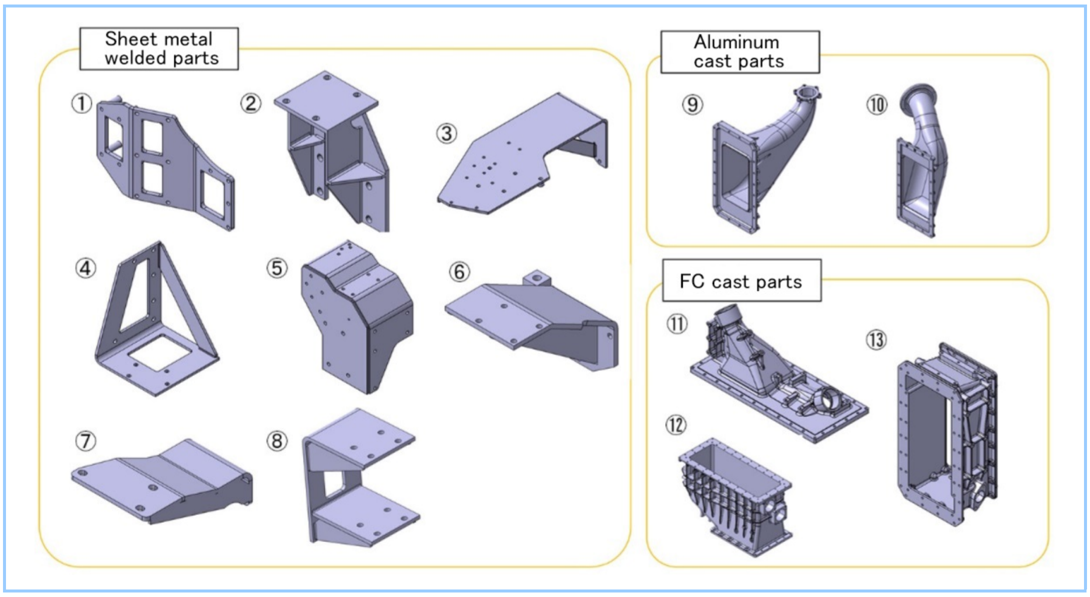

Figure 3 Parts for which correlation was made

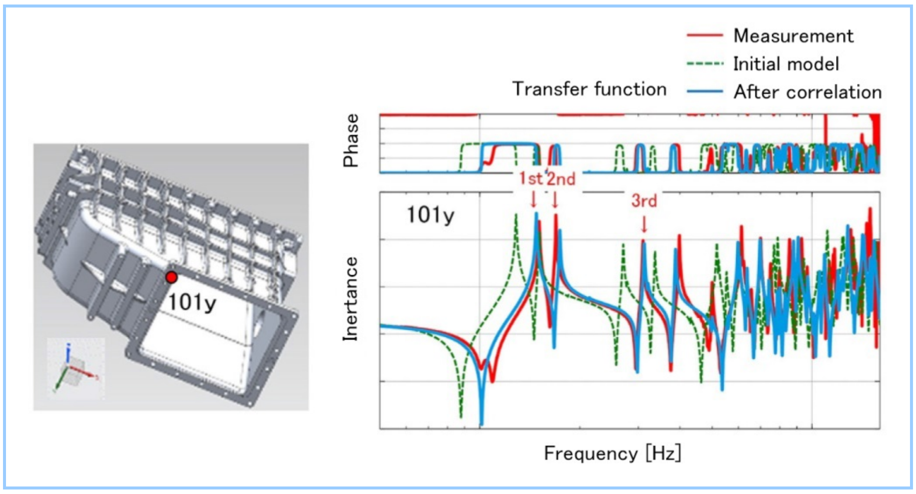

Figure 4 Step 1: Correlation example of individual part

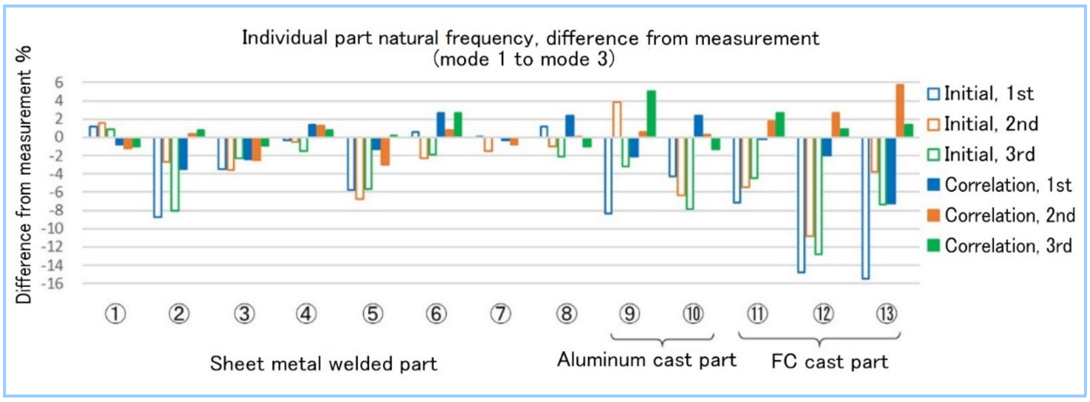

Figure 5 Step 1: Result example of correlation for individual parts (Comparison of individual part natural frequency with actual measurements)

Step 2: Next, we performed a hammering test on subassemblies with the parts coupled through bellows and O-rings and adjusted the spring constants of the coupling. **Figure 6** shows the correlation result for the coupling through bellows and **Figure 7** shows the correlation result for coupling through an O-ring. It is necessary to consider the low-rigidity bellows and O-rings as spring elements and to adjust them to the measured vibration characteristics.

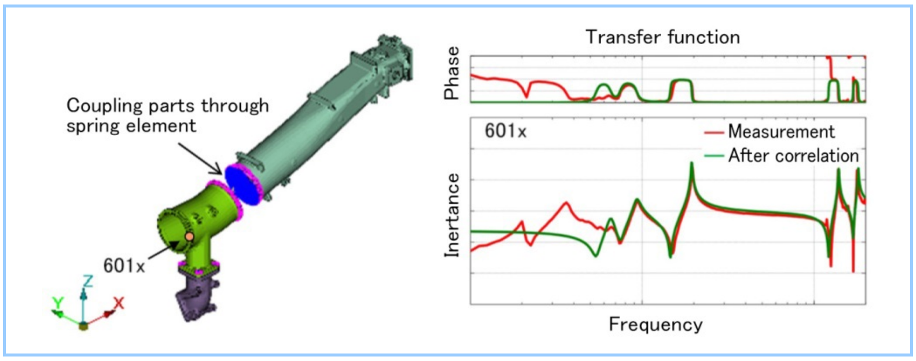

Figure 6 Step 2: Correlation of sub-assembly (coupling through bellows)

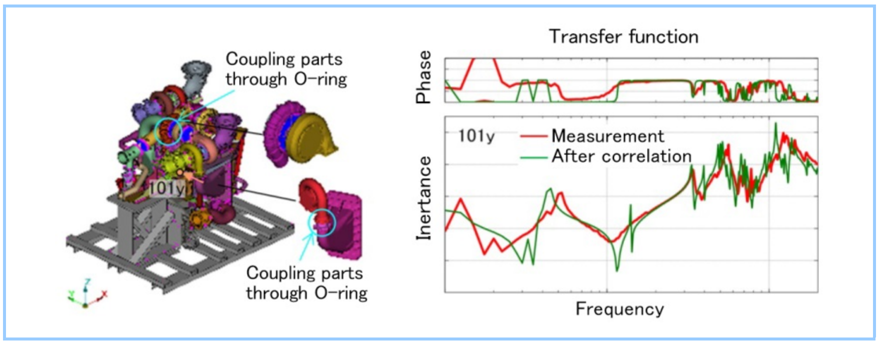

Figure 7 Step 2: Correlation of sub-assembly (coupling through O-ring)

Step 3: Finally, we performed the correlation of the spring constants of spring elements coupling the exhaust ducts and cooling water piping to the external piping so that the vibration analysis result matches the measured vibration levels in actual operation with the engine assembled to the generator set. As shown in **Figure 8**, the spring constants has a significant effect on the peak level of the full assembly vibration mode, so it is important to reflect the spring constants measured with the engine installed in the analytical model.

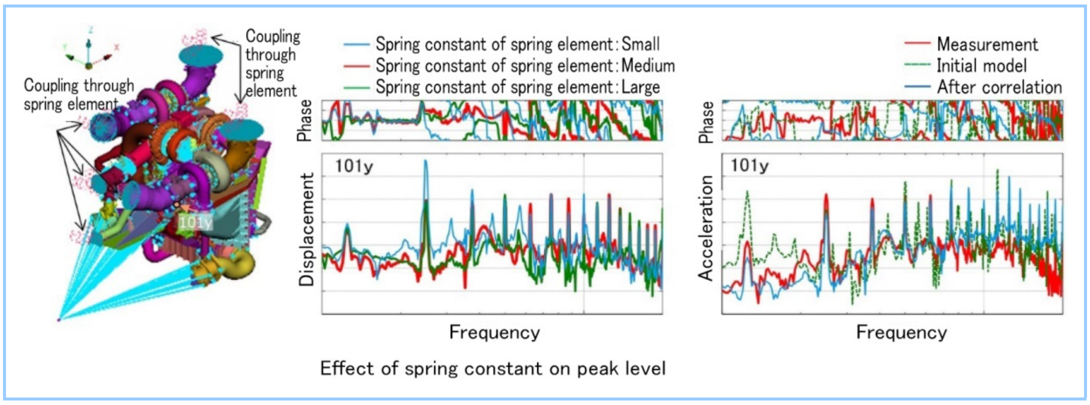

Figure 8 Step 3: Correlation of full-assembly

4. Calculation of analytical excitation force

Figure 9 shows the procedure for calculating the excitation force to be input to the assembly analysis based on the vibration measurement results during actual operation. We measured vibration data in three directions at four engine mounts (measurement positions were arbitrary) during actual operation, and estimated six-degree-of-freedom (three translational and three rotational directions) vibration at the engine center of gravity (an arbitrary virtual point) from the measured data. **Figure 10** shows a relational expression between the displacement vector {u} at the engine center of gravity and the displacement at each measurement point coordinate (four engine mount points). The displacement vector {u} was calculated using the least-squares method for the difference between the displacements at the four measurement points calculated by this equation and the actual measured values. The obtained displacement vector was input to the engine center of gravity as the excitation force for analysis.

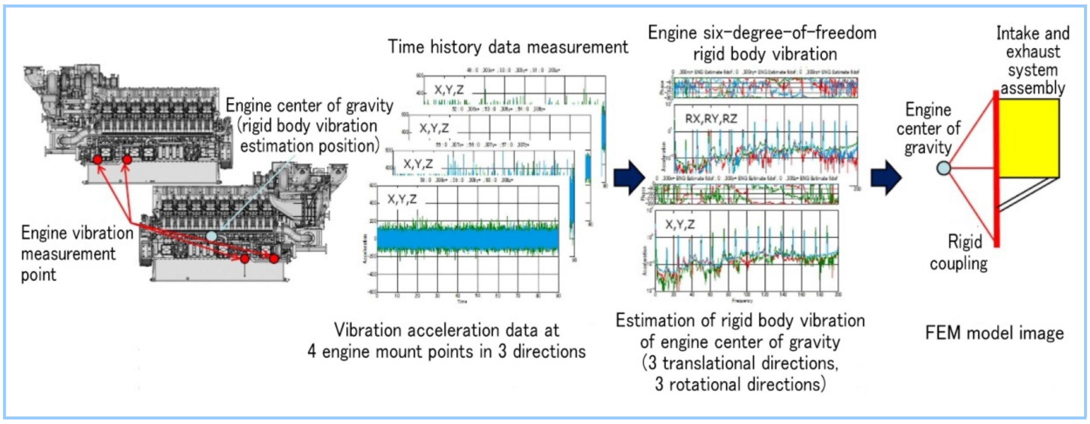

Figure 9　Calculation procedure for analytical vibration force

$$\begin{bmatrix} 1 & 0 & 0 & 0 & Z_1 & -Y_1 \\ 0 & 1 & 0 & -Z_1 & 0 & X_1 \\ 0 & 0 & 1 & Y_1 & -X_1 & 0 \\ & & & \vdots & & \\ 1 & 0 & 0 & 0 & Z_n & -Y_n \\ 0 & 1 & 0 & -Z_n & 0 & X_n \\ 0 & 0 & 1 & Y_n & -X_n & 0 \end{bmatrix} \{u\} = \begin{Bmatrix} x_1 \\ y_1 \\ z_1 \\ \vdots \\ x_n \\ y_n \\ z_n \end{Bmatrix}$$

Xn, Yn, Zn : n-th measurement point coordinates
xn, yn, zn : n-th measurement point translation displacement
$\{u\}$: Displacement vector at any point

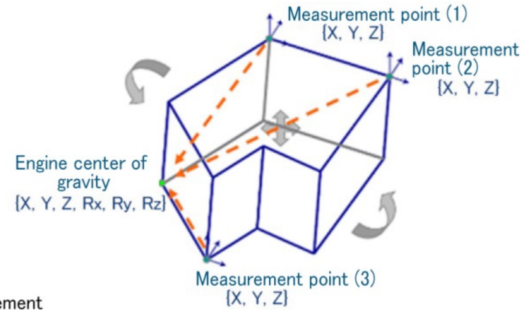

Estimate rigid body vibration of engine center of gravity using measured vibration data

Figure 10　Relational expression between displacement vector of virtual point and displacement of measurement point

This estimation assumes that the engine main body is a rigid body. We have ensured that the engine main body can be treated as a rigid body by using the obtained displacement vectors to back-calculate the displacements at the four measurement points and confirming that they are equivalent to the actual measured values.

With this method of calculating the excitation force, vibration analysis using a model which employs the FEM only on the intake and exhaust system assembly and couples the engine center of gravity and the intake and exhaust system assembly by rigid elements is allowed. In addition, since this method uses the least-squares method to calculate the excitation force, input conditions with no measurement error can be obtained.

5. Analysis accuracy verification result

Figure 11 shows the analysis result (displacement) using the displacement vector of the engine center of gravity estimated from the vibration measurement results during actual operation as input. It was verified that the application of the aforementioned accuracy improvement method resulted in the more accurate estimation of vibration characteristic measurements compared to the initial model. Also, the locations of high stress in each mode obtained from the analysis generally agreed with the damage locations that occurred in the actual equipment.

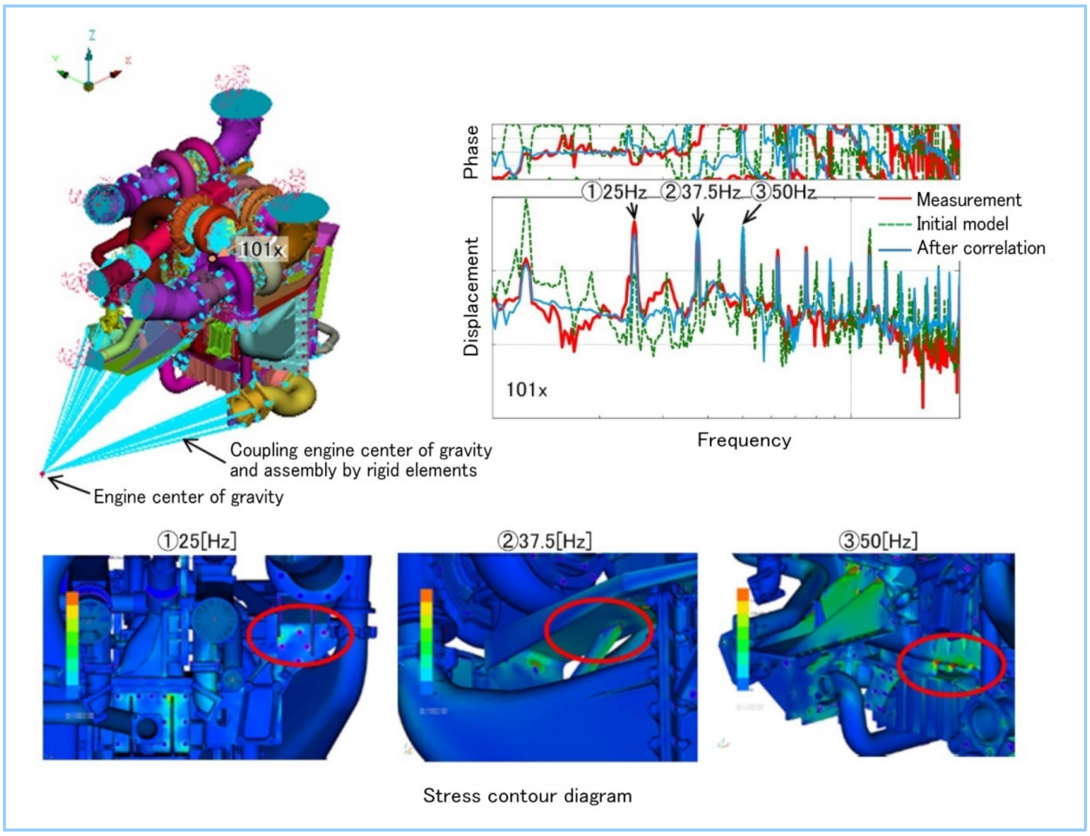

Figure 11　Analysis result of actual operation

6. FEM modeling guideline

Table 1 summarizes the FEM modeling guidelines based on the results obtained in these aforementioned efforts.

Moving forward, we will perform correlation and analysis in a similar way, accumulate practical values, and incorporate them into analytical modeling procedures.

Table 1　FEM modeling guidelines

<table>
<tr><th></th><th>Target part and coupling</th><th>Modeling</th><th>Density</th><th>Young's modulus</th><th>Spring constant and damping coefficient</th></tr>
<tr><td>1</td><td>Parts (machined parts)</td><td>Based on drawing</td><td rowspan="2">[Step 1] Material standard value
[Step 2] Value identified by correlation</td><td rowspan="3">Practical value (identified in this study)</td><td rowspan="3">—</td></tr>
<tr><td>2</td><td>Parts (sheet metal welded parts)</td><td>Based on drawing</td></tr>
<tr><td>3</td><td>Parts (cast parts)</td><td>Based on drawing</td><td>[Step 1] Material standard value x 1.1 (increase in actual wall thickness)
[Step 2] Correction by actual measured weight</td></tr>
<tr><td>4</td><td>Bellows</td><td rowspan="3">Spring element model</td><td rowspan="3">—</td><td rowspan="3">—</td><td rowspan="3">[Step 1] Practical value (identified in this study)
[Step 2] Value identified by correlation</td></tr>
<tr><td>5</td><td>O-rings</td></tr>
<tr><td>6</td><td>Support rigidity and damping of intake and exhaust system ducts</td></tr>
</table>

7. Conclusion

We found the following processes to be effective in improving the accuracy of vibration analysis of large-scale assemblies.

- Improving the accuracy of vibration characteristics of analytical models by hammering
- Reflecting the rigidity of connections to external piping when the engine is installed
- Estimation of analytical excitation force using measured vibration values during actual engine operation

By reflecting the values obtained in this study in analysis models for the new design of similar engine parts in the future as practical values, it is expected to improve the accuracy of the analysis in the design phase. Furthermore, we can achieve further improvement in the accuracy by performing correlation in the same way as the processes used in this study, feeding back the obtained values to analytical models, and accumulating practical values.

On the other hand, it is not efficient to perform hammering on all components of a large assembly, and so the challenge lies in the improvement of skills in selecting parts to be hammering-tested and in setting excitation positions for each part.